PHILOSOPHICAL TRANSACTIONS OF THE ROYAL SOCIETY A MATHEMATICAL, PHYSICAL & ENGINEERING SCIENCES

Computational mineral physics and the physical properties of perovskite

John P. Brodholt, A. R. Oganov and G. D. Price

Phil. Trans. R. Soc. Lond. A 2002 **360**, doi: 10.1098/rsta.2002.1078, published 15 November 2002

10.1098/rsta.2002.1078

THE ROYAL SOCIETY

Computational mineral physics and the physical properties of perovskite

By John P. Brodholt, A. R. Oganov and G. D. Price

Department of Earth Sciences, University College London, Gower Street, London WC1E 6BT, UK

Published online 27 September 2002

The inherent uncertainties in modern first-principles calculations are reviewed using geophysically relevant examples. The elastic constants of perovskite at lower-mantle temperatures and pressures are calculated using *ab initio* molecular dynamics. These are used in conjunction with seismic tomographic models to estimate that the lateral temperature contrasts in the Earth's lower mantle are 800 K at a depth of 1000 km, and 1500 K at a depth of 2000 km. The effect of Al^{3+} on the compressibility of $MgSiO_3$ perovskite is calculated using three different pseudopotentials. The results confirm earlier work and show that the compressibility of perovskites with Al^{3+} substituted for both Si^{4+} and Mg^{2+} is very similar to the compressibility of Al^{3+}-free perovskite. Even when 100% of the Si^{4+} and Mg^{2+} ions are replaced with Al^{3+}, the bulk modulus is only 7% less than that for Al^{3+}-free perovskite. In contrast, perovskites where Al^{3+} substitutes for Si^{4+} only and that are charge balanced by oxygen vacancies do show higher compressibilities. When corrected to similar concentrations of Al^{3+}, the calculated compressibilities of the oxygen-vacancy-rich perovskites are in agreement with experimental results.

Keywords: perovskite; lower mantle; *ab initio*; elastic constants; alumina

1. Introduction

The interpretation of one-dimensional seismological profiles of the Earth's mantle, such as PREM and AK135-f (Dziewonski & Anderson 1981; Kennett *et al.* 1995), and three-dimensional tomographic models (e.g. Kennett *et al.* 1998; Masters *et al.* 2000) in terms of chemistry, mineralogy and temperature is made difficult by the relative paucity of elastic data on lower-mantle minerals at simultaneously high temperatures and pressures. Uncertainties in the elastic properties of perovskite and magnesiowüstite as a function of temperature, pressure and composition mean that it is possible to propose many very different mineralogical and chemical models that fit the available seismological data for the Earth's lower mantle. For example, it has been shown that the lower mantle could be made exclusively of perovskite (e.g. Anderson 1983; Jeanloz & Knittle 1989; Stixrude *et al.* 1992), or that it has the same composition as the upper mantle (pyrolite) (e.g. Anderson 1997; Fiquet *et al.* 1998; Hama & Suito 2001; Jackson 1998; Stacey 1996) or that it is enriched in

One contribution of 14 to a Discussion Meeting 'Chemical reservoirs and convection in the Earth's mantle'.

iron and/or silicon with respect to the upper mantle (e.g. Bina & Silver 1990). It is clear that these different models imply very different evolutions, dynamics and structures for the Earth as a whole, and that producing accurate elastic constants (from which primary (P)- and secondary (S)-wave velocities can be obtained) is a pressing challenge for experimental and computational mineral physics.

Although experimental techniques are improving, it will be many years before accurate seismic properties of all the possible mantle phases (perovskite, magnesiowüstite, Ca-silicate perovskite, SiO_2-polymorphs, etc.) become available at mantle pressures and temperatures and span the full range of chemical composition. The importance of composition is highlighted particularly well by recent experiments and theoretical calculations showing that small amounts of Al^{3+} in $MgSiO_3$ perovskite have an unexpectedly large effect on its physical properties (Andrault *et al.* 2001; Brodholt 2000; Daniel *et al.* 2001; Zhang & Weidner 1999). It would seem that it is not enough to worry solely about the effect of Fe^{2+} on elastic moduli, the effects of Fe^{3+} and Al^{3+} may be just as important as the effects of temperature and Fe^{2+}.

While computational mineral physics techniques such as density-functional theory (DFT) have inherent uncertainties, as long as we understand and appreciate what they are it is possible to use these techniques in lieu of experimental data, particularly for extrapolation purposes. In this paper we will attempt to very briefly review modern DFT methods and to highlight these uncertainties. We will then present results on predicting the high-temperature and high-pressure elastic constants of $MgSiO_3$ perovskite, and the effect of Al^{3+} on the physical properties of perovskite.

2. *Ab initio* calculations and simulations

Although the details and methods of modern quantum-mechanical calculations have been reviewed many times, it is still worth highlighting the most important approximations used in our work. Hopefully this will help the non-specialist to develop a better appreciation of some of the inherent uncertainties, and with it a real appreciation of the strengths of these techniques. There are two classes of *ab initio* or first-principles calculations that have been applied to Earth materials; these are Hartree–Fock and DFT. Over the last five years or so, DFT seems to have become the choice for most calculations relevant to the deep Earth and so we will only discuss this here. We refer the interested reader to Jones & Gunnarsson (1989), Payne *et al.* (1992) and Pisani (1996) for detailed and rigorous descriptions of the methods and to Gillan (1997) for a somewhat friendlier, but still comprehensive, review.

(*a*) *Exchange–correlation*

The most important approximation made in most *ab initio* calculations is that concerning the interactions between electrons. Some parts are easy (e.g. the Hartree energy) but others are not. In particular the effects of exchange and correlation are difficult to deal with exactly. Correlation is exactly as it sounds: the motion of any particular electron is correlated to the motions of the other electrons in the system due to their Coulombic interactions. Although one can ignore correlation and just deal with a static average potential (as in the Hartree approximation), one cannot accurately describe bonding in this way. Exchange is an added term which leads naturally to the Pauli principle and says that if two electrons are exchanged, then

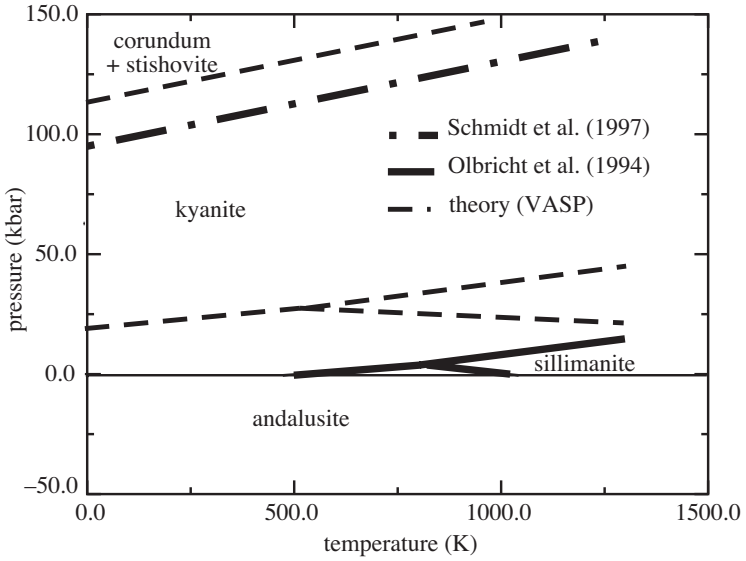

Figure 1. The phase diagram of the Al_2SiO_5 polymorphs predicted from *ab initio* calculations (Oganov & Brodholt 2000) compared with the experimental determination. Only the 0 K part of the theoretical phase diagram is calculated; the slopes are simply the experimental P–T slopes. Although the pressures of the predicted phase boundaries at 0 K are *ca.* 2–3 GPa too high, the order of the transition is correct. At the pressures of the lower mantle and core, an uncertainty of 2–3 GPa is generally acceptable.

the wave function must change sign. This adds another level of complexity, since we cannot treat the total N-electron wave function as simply the product of N one-electron wave functions; the total wave function is a much more complicated function of the one-electron wave functions. Attempting to solve Schrödinger's equation for the full N-electron system is basically a very serious N-body problem. All is not lost, however, since it can be rigorously shown that the problem can be incorporated into a single term called the exchange–correlation energy. Both correlation and exchange act to keep electrons apart and lower the energy of the system (relative to the Hartree approximation). If we knew this term exactly, we could find the exact solution to Schrödinger's equation for the real N-electron system. Unfortunately, the true exchange–correlation energy is not known for real systems and so we are forced to use approximations. This is the important point; it is the quality of these approximations that governs the quality of the results. The two main approximations are known as the local density approximation (LDA) and the generalized gradient approximation (GGA) and are discussed next.

(*b*) *LDA versus GGA*

It is not really necessary for the Earth scientist to know the details of these approximations; what is necessary, however, is an appreciation of their accuracy in predicting the properties of Earth-forming materials.

For calculating volumes and compressibilities of mineral phases, there is a rule of thumb that very often works (see Oganov & Brodholt 2000 and references therein).

The rule of thumb is that the LDA tends to underestimate volumes by 1% or 2% and overestimates the bulk modulus by *ca.* 10%, while the GGA tends to predict the opposite; volumes are overestimated by 1% or 2% and the bulk modulus is underestimated. Unfortunately this does not always hold and, in addition, there can be a fortuitous cancellation of errors with errors in the pseudopotential (discussed later). There is no way of knowing *a priori* exactly how accurate the method will be for any given system, and in the end one must compare it with all available experimental data to judge whether the calculation has the accuracy for one's particular needs. For instance, at high pressure the difference between the experimentally measured volume for hexagonally close-packed iron and that calculated with the GGA is *ca.* 1% (Vočadlo *et al.* 1997). At low pressures, however, the errors are substantially greater, although this may be due to subtle magnetic effects, not a failure of the GGA itself. For $MgSiO_3$ perovskite, our GGA calculations (discussed below) predict a zero-pressure volume of 168.0 $Å^3$, which is *ca.* 4% greater than the experimental value of 162.5 $Å^3$.

One can also use DFT calculations to predict phase diagrams but, as with equation of state calculations, there are uncertainties in the results that need to be considered. An example is given in figure 1 for the Al_2SiO_5 polymorphs (Oganov & Brodholt 2000). At zero temperature the predicted andalusite-to-kyanite transition is *ca.* 3 GPa higher than the experimental pressure. This has the unfortunate effect of making the wrong phase stable at the surface of the Earth, which would not be satisfactory if one were trying to predict the stable phase under ambient conditions. However, a 3 GPa uncertainty in the position of a phase boundary is not an excessive error when working at the pressures of the lower mantle or core. The breakdown of kyanite to the oxides is also *ca.* 2.5 GPa higher than the experimental value but, reassuringly, the progression of the stable phases with pressure is correct. Given that the 0 K part of the phase diagram was predicted using no experimental data other than a rough estimate of atomic coordinates of the phases and some fundamental constants, this must be regarded as a success.

(*c*) *Pseudopotentials*

Since there is a substantial computational burden for every electron in the system, a considerable advantage is gained in minimizing the number of electrons that are dealt with explicitly. In most cases, the major contribution to bonding comes from the valence electrons; the core electrons remain essentially the same in different chemical environments. This has led to a commonly used approximation in which the interactions of the valence electrons with the core electrons are represented by a pseudopotential. This is computationally much more tractable than calculating the true potential felt by the valence electrons. Although there are a number of different types of pseudopotentials, all modern pseudopotentials are generated in such a way as to match the wave function of the true all-electron atom outside of a prescribed core radius. The hope is to produce a pseudopotential that can then reproduce the properties of an all-electron calculation in different environments (i.e. it is transferable). This would then mean that all the error in the calculation is due to the exchange–correlation approximation. Unfortunately, as pointed out by Grinberg *et al.* (2001), and by Stixrude *et al.* (1998) for Earth materials, this is not always the case and different pseudopotentials can lead to different results (of the same order as the LDA error), so care must be taken.

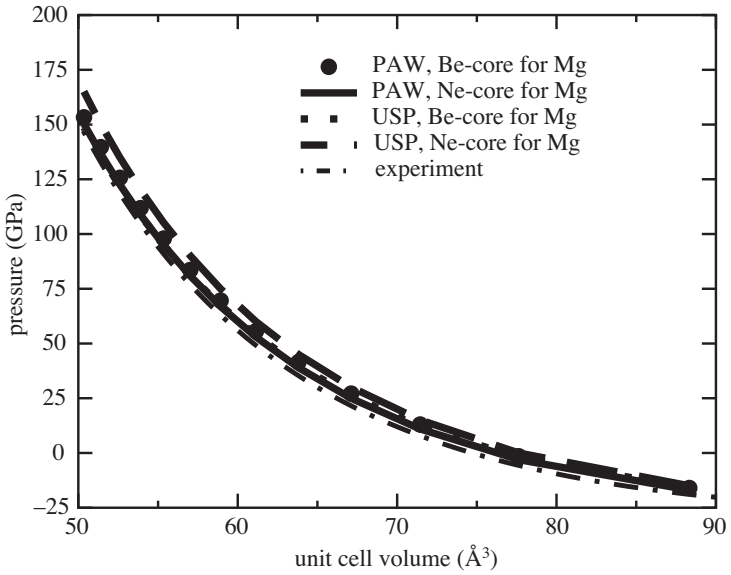

Figure 2. The predicted equation of state of MgO from two all-electron calculations (PAW) and two pseudopotential calculations (USP, ultrasoft pseudopotential), compared with the experimental equation of state. The pseudopotential that explicitly treats eight electrons (Be core) is identical to the all-electron calculations. The simpler Mg pseudopotential, which has a neon core and therefore treats only two electrons explicitly, is considerably worse.

Figure 2 shows the effects of two different pseudopotentials on the equation of state of MgO and compares them with experimental data and with two all-electron calculations using the projector augmented-wave (PAW) method (Blochl 1994; Kresse & Joubert 1999). The difference between the two pseudopotential calculations is in the number of electrons that are treated explicitly. As expected from GGA calculations, all the predicted volumes are somewhat larger than the experimental volume; however, the pseudopotential generated with a neon core is substantially worse than the other calculations. This is because it keeps more electrons in the core region than the one generated with a beryllium core, and so has fewer 'valence' electrons. The pseudopotential with the beryllium core gives results identical to the all-electron approach. Interestingly, we have performed a similar test on perovskite and find that, in contrast, the effect on the equation of state is far less than in MgO and that both cores give very similar results.

(*d*) *Ab initio molecular dynamics*

Until recently, *ab initio* calculations have generally been restricted to zero temperature (the 'athermal limit'), since it is computationally very expensive to treat temperature. In other words, we could only calculate the energetics and physical properties of static structures. The continual increase in computational power, however, now means that the effect of temperature can be explicitly included and *ab initio* molecular dynamics can now be almost routinely applied to geophysical problems. As in real systems, atoms in a molecular-dynamics simulation move through time, being acted on by forces from the other atoms in the system. By averaging

Table 1. *Calculated and experimental elastic constants of* $MgSiO_3$ *perovskite*

	0 GPa		38 GPa		88 GPa	
C_{ij}	0 K (calc.)	0 K (exp.)	1500 K	2500 K	1500 K	3500 K
C_{11}	493	482	616	579	826	783
C_{22}	546	537	711	654	991	878
C_{33}	470	485	663	615	945	850
C_{12}	142	144	280	258	477	431
C_{13}	146	147	249	243	362	356
C_{23}	160	146	264	265	396	395
C_{44}	212	204	262	232	336	270
C_{55}	186	186	219	210	266	234
C_{66}	149	147	199	178	264	195

values collected as a function of time one can obtain a value for the desired property at the temperature of the simulation (i.e. the average kinetic energy gives the temperature of the simulation). Molecular dynamics (MD) has traditionally been used with empirical potentials, whereby the forces between the constituent atoms are described beforehand—either by fitting to some experimental data or from *ab initio* calculations on a static structure. This has the benefit of being cheap, and very large systems can be simulated (millions or even billions of atoms). The drawback is that it is generally difficult to produce empirical potentials that correctly describe interactions in different systems. For instance, a potential that describes the interaction between silicon and oxygen ions in forsterite may not work well for interactions between the same pair of ions in perovskite. In other words, it is difficult to 'transfer' a given set of empirical parameters.

In *ab initio* molecular dynamics, the forces are calculated with a first-principles calculation at each time-step. Although expensive, and so restricted to a few hundred or so atoms, it is clearly the method of choice for complicated systems, as it includes an explicit account of the quantum nature of the electronic structure and so should be free from problems of transferability that are inherent in traditional MD.

3. The high-temperature elastic constants of perovskite

The equation of state and thermoelasticity of $MgSiO_3$ perovskite are still relatively poorly known. In particular, the only published elastic constants for perovskite have been measured under room conditions only (Yeganeh-Haeri 1994). Even when high-pressure and high-temperature experimental data exist, there are some quite considerable differences between them. For instance, at 1000 K, zero-pressure experimental thermal expansivites differ by a factor of two (see Anderson 1998; Oganov *et al.* 2001*a*). We have, therefore, used state-of-the-art *ab initio* MD to calculate the high-temperature and high-pressure thermoelastic properties of perovskite.

As mentioned above, the GGA tends to overestimate volumes and underestimate the bulk modulus for most, but not all, phases. This, unfortunately, is also true for our calculations on $MgSiO_3$ and is therefore a problem for providing accurate elastic properties. (See Karki *et al.* (2001) for a comparison of different theoretical results

and experiment.) Fortunately, as shown by Oganov *et al.* (2001*a*), this can be corrected for by making a small constant adjustment of 12.08 GPa in pressure. Although use of an empirical correction is not ideal, the constant-pressure correction results in an almost perfect agreement of the calculated cell parameters, the bulk modulus, and the nine elastic constants with the experimental results (see table 1). We have, therefore, applied this same correction when calculating the high-temperature elastic constants (C), which are given in table 1. The exact details of the calculations can be found in Oganov *et al.* (2001*b*). We believe that these are the best estimates of high-temperature elastic properties of $MgSiO_3$ perovskite available.

We can immediately use our results to evaluate the estimates of the temperature dependence of P- and S-wave velocities used by Forte & Mitrovica (2001) in their analyses of the thermal structure of the core–mantle boundary (CMB) from tomography. These derivatives were based on an equation-of-state analysis of Jackson (1998). Using our values for the elastic constants we obtain $\partial \ln V_\mathrm{P}/\partial T = -2.5 \times 10^{-5}\ \mathrm{K}^{-1}$ and $\partial \ln V_\mathrm{S}/\partial T = -3.7 \times 10^{-5}\ \mathrm{K}^{-1}$ at 38 GPa. At 88 GPa we obtain $\partial \ln V_\mathrm{P}/\partial T = -2.0 \times 10^{-5}\ \mathrm{K}^{-1}$ and $\partial \ln V_\mathrm{S}/\partial T = -3.8 \times 10^{-5}\ \mathrm{K}^{-1}$. These values compare with $\partial \ln V_\mathrm{P}/\partial T = -2.2 \times 10^{-5}\ \mathrm{K}^{-1}$ and $\partial \ln V_\mathrm{S}/\partial T = -4.7 \times 10^{-5}\ \mathrm{K}^{-1}$ used by Forte & Mitrovica (2001) for the anharmonic part of the derivatives at the CMB. The temperature variation of V_P is in good agreement, while our estimate for the temperature effect on the S-wave velocities is significantly smaller than that used by Forte & Mitrovica (2001).

The elastic constants can be used in conjunction with bulk sound-speed tomographic models to estimate lateral temperature variations in the lower mantle by assuming that all the tomographic variations in the bulk sound velocity are due to temperature. This is a reasonable assumption since anelasticity only affects the shear modulus, and chemical composition only weakly affects the bulk modulus. Using our calculated bulk sound velocities and the bulk-sound-velocity tomographic model of Masters *et al.* (2000), we obtain a temperature difference between the hottest and coldest mantle of 800 K at a depth of 1000 km, and 1500 K at a depth of 2000 km. These values would be considerably reduced to *ca.* 500 K and 1000 K at depths of 1000 and 2000 km, respectively, if the bulk-sound-velocity model of Kennett *et al.* (1998) is used instead. Kesson *et al.* (1998) estimated that subducting slabs would have to be *ca.* 650 K cooler than the surrounding mantle to be neutrally buoyant at the CMB, but *ca.* 850 K cooler for them to have been sufficiently dense to reach there. Extrapolating our maximum temperature contrasts to the CMB gives a *ca.* 1500–2000 K difference between the hottest and coldest parts of the CMB (again depending on which tomographic model is used). We predict that the cool regions will be somewhere between 750 K and 1000 K cooler than the surrounding mantle (i.e. one-half of the maximum variation). These temperature contrasts indicate that slabs are likely to have enough negative buoyancy to reach the CMB.

The covariation in P- and S-wave velocities at a particular pressure is given by the parameter

$$R_P = \left(\frac{\partial \ln V_\mathrm{S}}{\partial \ln V_\mathrm{P}}\right)_P.$$

This is a useful parameter since it has a relatively restricted range of 0.9–1.44 for mantle phases on which it has been measured or estimated (Anderson & Isaak 1995; Karato & Karki 2001). The observed range in the lower mantle is, however, much

larger and increases from *ca.* 1.7 to 2.6 between depths of 1000 and 2000 km (Robertson & Woodhouse 1995) (although the exact value depends on the particular tomographic model and may be as high as 3.2). Using our calculated elastic constants (which include anharmonic effects), we obtain a value for R_P of 1.5 at 1000 km and 1.9 at 2000 km. This is consistent with other anharmonic estimates that show it increasing from 1.5 to 2.1 in the lower mantle (Karato & Karki 2001).

The discrepancy between the mineralogical results (1.5–1.9) and the much higher seismological observations (2.6–3.2) must be due to either anelastic effects or lateral chemical heterogeneity. Anelasticity may be able to account for most of the discrepancy, but this depends on the activation energy used for the relaxation process (Karato & Karki 2001). To evaluate the effect of lateral chemical heterogeneity, we need seismic properties as a function of composition. As iron is the next most abundant element in perovskite after Mg, O and Si, we need accurate determinations of $\partial \ln V_{S,P}/\partial X_{Fe}$ for both perovskite and magnesiowüstite (this is ongoing work). However, as described in the next section, Al^{3+} may be just as important.

4. The effect of aluminium on the elastic properties of perovskite

In last three years, considerable attention has been paid to the effect of small amounts of alumina on the physical properties of $MgSiO_3$ perovskite. It was found by Zhang & Weidner (1999) that only 5 wt% Al_2O_3 in perovskite reduces its bulk modulus by *ca.* 10%. This was subsequently confirmed by Daniel *et al.* (2001). This is an unusually large effect on the bulk modulus for such a small difference in chemical composition. For comparison, experiments on $MgSiO_3$ perovskites with Fe^{2+}/Mg^{2+} ratios between 0.0 and 0.2 showed that its bulk modulus is essentially independent of iron content (Mao *et al.* 1991). It was suggested by Navrotsky (1999) that the large effect from Al^{3+} may be due to a high concentration of oxygen vacancies formed to charge balance the substitution of Al^{3+} for Si^{4+} in the octahedral site.

In order to test this idea, *ab initio* calculations were performed on two end-member Al-bearing perovskites (Brodholt 2000). The first was a brownmillerite structure, where all the Al^{3+} substitutes for Si^{4+} charge balanced by oxygen vacancies ($Mg_2Al_2O_5$), and the second end member had Al^{3+} substituted for both Si^{4+} and Mg^{2+}. The second mechanism does not need oxygen vacancies for charge balance. The compressibilities of these two Al-bearing perovskites were then compared with pure $MgSiO_3$ perovskite, and it was found that only the brownmillerite-type substitution mechanism shows an increased compressibility; when Al^{3+} is incorporated into both the octahedral Si-site and the larger site normally occupied by Mg, the compressibility is almost identical to pure $MgSiO_3$. This is consistent with the suggestion of Navrotsky (1999) that the anomalous compressibility is due to oxygen vacancies.

By calculating the enthalpy of a reaction between the two end-member Al-bearing perovskites, it was also found that the oxygen-vacancy mechanism is only stable at pressures up to *ca.* 30 GPa (Brodholt 2000). At higher pressures the vacancy-free mechanism became favoured. This suggested that there may be a zone of 150 km or so in the top of the lower mantle with very different physical properties from the rest of the lower mantle below. As discussed later, this may have important geophysical implications.

More recently Andrault *et al.* (2001) published the results of diamond-anvil experiments on alumina-bearing perovskites that are radically different from the experimental and theoretical results discussed above. They found that at high pressures and temperatures aluminous perovskites are actually *ca.* 10% *less* compressible than aluminous-free perovskites; this is completely opposite from the findings of Zhang & Weidner (1999) and Daniel *et al.* (2001). Since their samples were equilibrated at higher pressures and temperatures than those of the earlier experiments, they suggest that the synthesis conditions were outside the stability of the oxygen-vacancy mechanism. Although this is an appealing interpretation of the experimental data, the compressibilities of the vacancy-free aluminous perovskites calculated by Brodholt (2000) are almost exactly the same as the pure $MgSiO_3$ perovskites. They do not show the strong decrease in compressibility found by Andrault *et al.* (2001). Since the observed decrease in compressibility is of the order of the increased compressibility found by Zhang & Weidner (1999) that has generated so much interest, it would, if correct, have similarly important geophysical implications. We have therefore revisited this in order to see if we can resolve why the *ab initio* calculations do not show any decrease in compressibility with increasing alumina content.

Figure 3 depicts a perovskite structure where one-quarter of the Mg atoms and one-quarter of the Si atoms have been replaced by Al atoms. This yields a unit cell with the composition $(Mg_3Al)(Si_3Al)O_{12}$. This is a far higher concentration of Al^{3+} than in the experimental samples, and so we would expect it to magnify any effect on the compressibility. Although for one unit cell with periodic boundary conditions there are two distinct ways of arranging the two Al atoms in the two different sites, the difference in energy and volumes between them is negligible (less than 2 meV and 0.08 $Å^3$ per unit cell) and so we will only consider one of them.

To model the oxygen-vacancy mechanism, we again use the brownmillerite structure used by Brodholt (2000). This is the end member of a homologous series of oxygen-deficient perovskites that can range from one in six oxygens being vacant to an arbitrarily small concentration. All the octahedral sites normally occupied by Si are now occupied by Al, and the larger 8-12 site is occupied by Mg as usual. The removal of one in six oxygens means that 50 were coordinated.

Figure 4 shows the compressibilities of the two aluminous-bearing perovskites together with the compressibility of Al-free $MgSiO_3$ perovskite. We have used three different pseudopotentials to make absolutely sure that the results are not biased by the choice of pseudopotential. The first set (Old USP) are those supplied with CASTEP and used by Brodholt (2000). The second set (New USP) are new pseudopotentials for oxygen and aluminium derived by B. Civalleri and N. M. Harrison in 2000.† These are more reliable than the older pseudopotentials and give very good agreement with all-electron calculations on silica and alumina polymorphs. The third set are from the VASP catalogue of pseudopotentials, which have been well tested over a range of conditions.

The compressibilities of the $MgSiO_3$ perovskite and the $(Mg_3Al)(Si_3Al)O_{12}$ perovskite calculated with the three pseudopotentials are very similar; only the brownmillerite structure shows an effect of the pseudopotential on the compressibility, with the newer pseudopotentials giving a slightly more compressible structure than the other two. It is not clear why only the brownmillerite is affected, since, except for

† See http://www.cse.dl.ac.uk/Activity/UKCP+1080/ for more information.

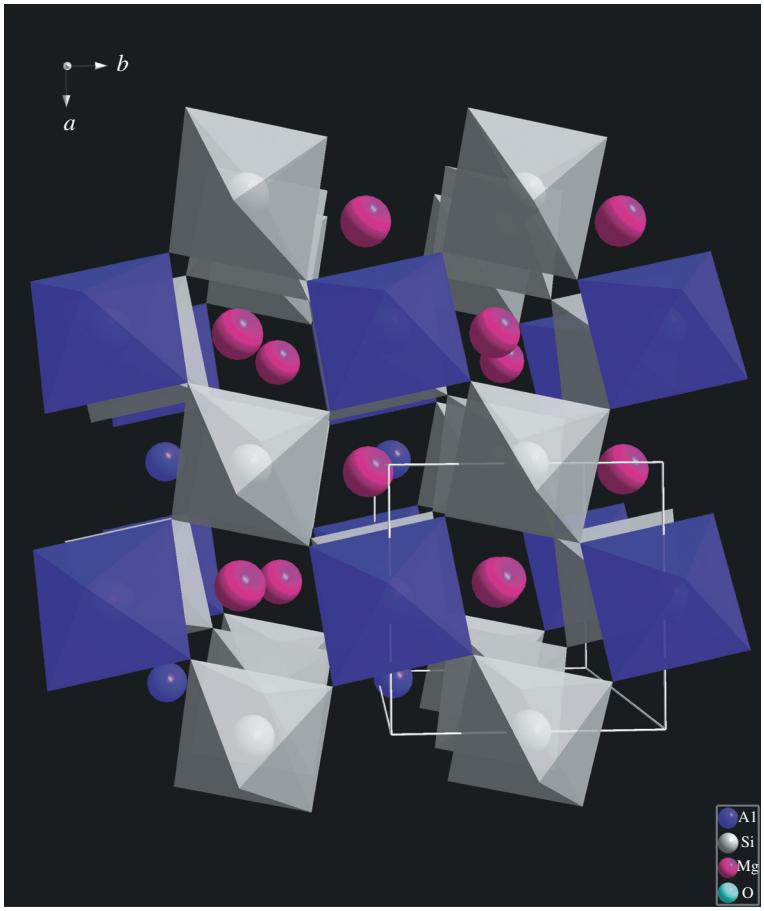

Figure 3. The structure of perovskite with one Al^{3+} substituting for Si^{4+} and one for Mg^{2+} in each unit cell.

the tetrahedral Al^{3+}, the atomic coordinations are similar to the other perovskite structures. It may be that the structure is developing a dynamical instability at very high pressures, which may explain why the third-order Birch–Murnaghan fit is not particularly good. (See Oganov *et al.* (2001*c*) for an example of EOS poorly fitted by conventional analytical formulae near a phase transition.)

Nevertheless, these results add support to those of Brodholt (2000), showing that the compressibility of the Al-bearing $(Mg_3Al)(Si_3Al)O_{12}$ perovskite with no vacancies is very similar to the Al-free perovskite (218 GPa versus 227 GPa when $K'((\partial K/\partial P)_T)$ is fixed at 4, or 233 and 240 when K' is allowed to vary). Given that this is for a very high concentration of Al, this sort of substitution mechanism cannot account for the 10% increase in compressibility found experimentally (Daniel *et al.* 2001; Zhang & Weidner 1999) for only 5% Al_2O_3. In contrast, the brownmillerite structure does show an increased compressibility, supporting the suggestion that the experimental samples have a high concentration of oxygen vacancies.

It is also clear that the calculations do not explain the very strong decrease in compressibility found by Andrault *et al.* (2001). We have looked at this further by

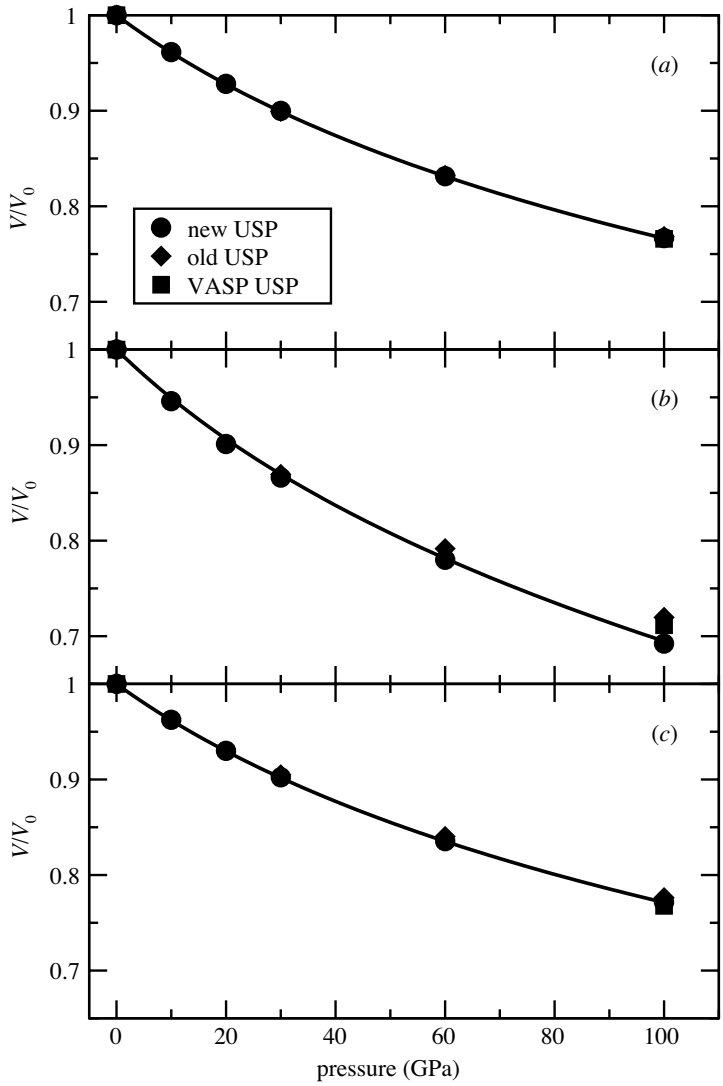

Figure 4. The compressibility of (*a*) the perovskite shown in figure 3, (*b*) $Mg_2Al_2O_5$ brownmillerite and (*c*) $MgSiO_3$ perovskite, as calculated with three different pseudopotentials (see text). Only the compressibility of brownmillerite is affected by the choice of pseudopotential. Nevertheless, it is clear that only the brownmillerite structure is more compressible that $MgSiO_3$ perovskite. Substituting Al^{3+} for Si^{4+} and Mg^{2+} has only a very small effect on the compressibility.

calculating the compressibility of a pure Pbnm Al_2O_3 perovskite. This represents a 100% substitution of Al into both the 8-12 Mg site and the octahedral Si site. For this we find a bulk modulus of 211 GPa for a K' of 4 and 223 when K' is allowed to vary (these results agree nicely with the LDA results of Duan *et al.* (1998)). The compressibility of this end member is still greater (by *ca.* 7%) than the $MgSiO_3$ perovskite, and so we conclude that neither the increased compressibility found by Zhang & Weidner (1999) and Daniel *et al.* (2001) nor the decreased compressibility at

higher pressure found by Andrault *et al.* (2001) can be explained by a substitution of Al into both Mg and Si sites. The increased compressibility is consistent with an oxygen-vacancy mechanism, but we can offer no explanation for the decreased compressibility found experimentally at higher pressures by Andrault *et al.* (2001).

5. Discussion

The high-temperature and high-pressure elastic constants of $MgSiO_3$ perovskite obtained from DFT calculations are essential for properly interpreting the observed seismic properties of the Earth's mantle. However, these are not enough; we also need to know the effects of composition and anelasticity. Although the effect of iron content on both the shear and compressional moduli is thought to be small in comparison with temperature (Forte & Mitrovica 2001; Jackson 1998), the very strong effect that Al has on the compressibility of perovskite suggests that it will have an even more marked effect on the shear moduli. In addition, even small concentrations of ionic vacancies would strongly affect many other physical properties, particularly the transport properties such as diffusion and creep. Using geoid inversions, Zhang & Christensen (1993), Kido & Cadek (1997) and Kido *et al.* (1998) have proposed that there is a low-viscosity zone under the transition zone. We suggest that a perovskite with a high concentration of vacancies can provide a physical mechanism for this. A low-viscosity zone in the lower mantle would have important geodynamical implications. For example, Cizkova *et al.* (1999) have shown that with such a low-viscosity layer it is possible to produce cold thermal anomalies in the lower mantle beneath subducting slabs even when there is no mass transfer between the upper and lower mantle. These modelled thermal anomalies are visually similar to those interpreted in tomographic models as slabs penetrating into the lower mantle. Instead of being caused by colder material flowing into the lower mantle, the modelled anomalies are the result of cooling from the subducting slab, which remains in the upper mantle. For this to occur, the flow in the upper and lower mantle must be decoupled by some sort of low-viscosity channel *ca.* 660 km deep. We are well aware that the evidence for whole-mantle convection is compelling and we are not necessarily arguing for layered convection. We are, however, emphasizing that perovskites have a rich crystal chemistry and may yet throw up surprises with fundamental geophysical implications.

References

Anderson, D. L. 1983 Chemical compostion of the mantle. *J. Geophys. Res.* **88**, B41–B52.

Anderson, O. L. 1997 Finding the isentropic density of perovskite: implications for iron concentrations in the lower mantle. *Geophys. Res. Lett.* **24**, 213–216.

Anderson, O. L. 1998 Themoelastic properties of $MgSiO_3$ perovskite using the Debye approach. *Am. Mineralogist* **83**, 23–35.

Anderson, O. L. & Isaak, D. G. 1995 Elastic constants of mantle minerals at high temperatures. In *Mineral physics and crystallography* (ed. T. J. Ahrens). AGU Reference Shelf Series, vol. 2, pp. 64–97. Washington, DC: American Geophysical Union.

Andrault, D., Bolfan-Casanova, N. & Guignot, N. 2001 Equation of state of lower mantle (Al, Fe)-$MgSiO_3$ perovskite. *Earth Planet. Sci. Lett.* **193**, 501–508.

Bina, C. R. & Silver, P. G. 1990 Constraint on lower mantle compostion and temperature from density and bulk sound velocity profiles. *Geophys. Res. Lett.* **17**, 1153–1156.

Blochl, P. E. 1994 Projector augmented-wave method. *Phys. Rev.* B **50**, 17 953–17 979.

Brodholt, J. P. 2000 Pressure-induced changes in the compression mechanism of aluminous perovskite in the Earth's mantle. *Nature* **207**, 620–622.

Cizkova, H., Cadek, O., van den Berg, A. P. & Vlaar, N. J. 1999 Can lower mantle slab-like seismic anomalies be explained by thermal coupling between the upper and lower mantles? *Geophys. Res. Lett.* **26**, 1501–1504.

Daniel, I., Cardon, H., Fiquet, G., Guyot, F. & Mezouar, M. 2001 Equation of state of Al-bearing perovskite to lower mantle pressure conditions. *Geophys. Res. Lett.* **28**, 3789–3792.

Duan, W., Wentzcovitch, R. M. & Thomson, K. T. 1998 First-principles study of high-pressure alumina polymorphs. *Phys. Rev.* B **57**, 10 363–10 369.

Dziewonski, A. M. & Anderson, D. L. 1981 Preliminary reference Earth model. *Phys. Earth Planet. Inter.* **25**, 297–356.

Fiquet, G., Andrault, D., Dewaele, A., Charpin, T., Kunz, M. & Hausermann, D. 1998 *P–V–T* equation of state of $MgSiO_3$ perovskite. *Phys. Earth Planet. Inter.* **105**, 21–31.

Forte, A. M. & Mitrovica, J. X. 2001 Deep-mantle high-viscosity flow and thermochemical structure inferred from seismic and geodynamic data. *Nature* **410**, 1049–1056.

Gillan, M. J. 1997 The virtual matter laboratory. *Contemp. Phys.* **38**, 115–130.

Grinberg, I., Ramer, N. J. & Rappe, A. M. 2001 Quantitative criteria for transferable pseudopotentials in density functional theory. *Phys. Rev.* B **63**, 201102.

Hama, J. & Suito, K. 2001 Thermoelastic models of minerals and the composition of the Earth's lower mantle. *Phys. Earth Planet. Inter.* **125**, 147–166.

Jackson, I. 1998 Elasticity, composition and temperature of the Earth's lower mantle: a reappraisal. *Geophys. J. Int.* **134**, 291–311.

Jeanloz, R. & Knittle, E. 1989 Density and composition of the lower mantle. *Phil. Trans. R. Soc. Lond.* A **328**, 377–389.

Jones, R. O. & Gunnarsson, O. 1989 The density functional formulism, its applications and prospects. *Rev. Mod. Phys.*, **61**, 689–746.

Karato, S. & Karki, B. B. 2001 Origin of lateral heterogeneity of seismic wave velocities and density in the deep mantle. *J. Geophys. Res.* **106**, 21771–21783.

Karki, B., Stixrude, L. & Wentzcovitch, R. 2001 High-pressure elastic properties of major materials of the Earth's mantle from first principles. *Rev. Geophys.* **39**, 507–534.

Kennett, B. L. N., Engdahl, E. R. & Buland, R. 1995 Constraints on seismic velocities in the Earth from travel-times. *Geophys. J. Int.* **122**, 108–124.

Kennett, B. L. N., Widiyantoro, S. & van der Hilst 1998 Joint seismic tomography for bilk sound and shear wave speed in the Earth's mantle. *J. Geophys. Res.* **103**, 12 469–12 493.

Kesson, S. E., Gerald, J. D. F. & Shelley, J. M. 1998 Mineralogy and dynamics of a pyrolite lower mantle. *Nature* **393**, 252–255.

Kido, M. & Cadek, O. 1997 Inferences of viscosity from the oceanic geoid: indication of a low viscosity zone below the 660 km discontinuity. *Earth Planet. Sci. Lett.* **151**, 125–137.

Kido, M., Yuen, D. A., Cadek, O. & Nakakuki, T. 1998 Mantle viscosity derived by genetic algorithm using oceanic geoid and seismic tomography for whole-mantle versus blocked-flow situations. *Earth Planet. Sci. Lett.* **107**, 307–326.

Kresse, G. & Joubert, D. 1999 From ultrasoft pseudopotentials to the projector augmented-wave method. *Phys. Rev.* B **59**, 1758–1775.

Mao, H. K., Hemley, R. J., Fei, Y., Shu, J. F., Chen, L. C., Jephcoat, A. P. & Wu, Y. 1991 Effect of pressure, temperatures, and compostion on lattice parameters and density of (Fe, Mg)SiO_3-perovskites to 30 GPa. *J. Geophys. Res.* **96**, 8069–8079.

Masters, G., Laske, G., Bolton, H. & Dziewonski, A. 2000 The relative behaviour of shear velocity, bulk sound speed, and compressional velocity in the mantle: implications for chemical and thermal structure. In *Earth's deep interior: mineral physics and tomography from the atomic to the global scale*. AGU Monographs, vol. 117, pp. 63–87.

Navrotsky, A. 1999 A lesson from ceramics. *Science* **284**, 1788–1789.

Oganov, A. R. & Brodholt, J. P. 2000 High-pressure phases in the Al_2SiO_5 system and the problem of aluminous phase in the Earth's lower mantle: *ab initio* calculations. *Phys. Chem. Miner.* **27**, 430–439.

Oganov, A. R., Brodholt, J. P. & Price, G. D. 2001*a* *Ab initio* elasticity and thermal equation of state of $MgSiO_3$ perovskite. *Earth Planet. Sci. Lett.* **184**, 555–560.

Oganov, A. R., Brodholt, J. P. & Price, G. D. 2001*b* The elastic constants of $MgSiO_3$ perovskite at pressures and temperatures of the earth's mantle. *Nature* **411**, 934–937.

Oganov, A. R., Price, G. D. & Brodholt, J. P. 2001*c* Theoretical investigation of metastable Al_2SiO_5 polymorphs. *Acta Crystallogr.* A **57**, 548–557.

Payne, M. C., Teter, M. P., Allan, D. C., Arias, T. & Joannopoulos, J. D. 1992 Iterative minimization techniques for ab-initio total energy calculations: molecular dynamics and conjugate gradients. *Rev. Mod. Phys.* **64**, 1045–1097.

Pisani, C. 1996 *Ab initio approaches to the quantum-mechanical treatment of periodic systems.* Lecture Notes in Chemistry, vol. 67, pp. 47–75. Springer.

Robertson, G. S. & Woodhouse, J. H. 1995 Evidence for proportionality of p and p heterogeneity in the lower mantle. *Geophys. J. Int.* **123**, 85–116.

Stacey, F. D. 1996 Thermoelasticity of (Mg, Fe)SiO_3 perovskite and a comparison with the lower mantle. *Phys. Earth Planet. Inter.* **98**, 65–77.

Stixrude, L., Hemley, R. J., Fei, Y. & Mao, H. K. 1992 Thermoelasticity of silicate perovskite and magnesiowüstite and stratification in the Earth's mantle. *Science* **257**, 1099–1101.

Stixrude, L., Cohen, R. E. & Hemley, R. J. 1998 Theory of minerals at high pressure. *Rev. Mineral.* **37**, 631–679.

Vočadlo, L., de Wijs, G., Kresse, G., Gillan, M. J. & Price, G. D. 1997 First principles calculations on crystalline and liquid iron at Earth's core conditions. *Faraday Discuss.* **106**, 205–217.

Yeganeh-Haeri, A. 1994 Synthesis and re-investigation of the elastic properties of single-crystal magnesium silicate perovskite. *Phys. Earth Planet. Inter.* **87**, 111–121.

Zhang, S. X. & Christensen, U. 1993 Some effects of lateral viscosity variations on geoid and surface velocities induced by density anomalies in the mantle. *Geophys. J. Int.* **114**, 531–547.

Zhang, J. & Weidner, D. J. 1999 Thermal equation of state of aluminium-enriched silicate perovskite. *Science* **284**, 782–784.